Scientific Research Publishing

Materials Sciences and Applications, 2022, 13, 603-626
https://www.scirp.org/journal/msa
ISSN Online: 2153-1188
ISSN Print: 2153-117X

Development of Sensible Heat Storage Materials Using Sand, Clay and Coal Bottom Ash

Boubou Bagre[1,2], Ibrahim Kolawole Muritala[3], Tizane Daho[2], Makinta Boukar[1], Yomi Woro Gounkaou[2], Babajide Epe Shari[1], Aissatou Ndiaye[1], Antoine Bere[2], Adamou Rabani[1]

[1]Doctoral Research Program-Climate Change and Energy, Université Abdou Moumouni (WASCAL-DRP-CCE), Niamey, Niger
[2]Laboratoire de Physique et de Chimie de l'Environnement, Université Joseph KI-ZERBO, Ouagadougou, Burkina Faso
[3]Institute of Low-Carbon Industrial Processes, German Aerospace Center (DLR), Zittau, Germany
Email: bagre.b@edu.wascal.org

How to cite this paper: Bagre, B., Muritala, I.K., Daho, T., Boukar, M., Gounkaou, Y.W., Shari, B.E., Ndiaye, A., Bere, A. and Rabani, A. (2022) Development of Sensible Heat Storage Materials Using Sand, Clay and Coal Bottom Ash. *Materials Sciences and Applications*, **13**, 603-626.
https://doi.org/10.4236/msa.2022.1312038

Received: November 8, 2022
Accepted: December 26, 2022
Published: December 29, 2022

Abstract

In this paper, the mechanical and thermal properties of a sand-clay ceramic with additives coal bottom ash (CBA) waste from incinerator coal power plant are investigated to develop an alternative material for thermal energy storage (TES). Ceramic balls are developed at 1000˚C and 1060˚C using sintering or firing method. The obtained ceramics were compressed with a compression machine and thermally analyse using Decagon devise KD2 Pro thermal analyser. A muffle furnace was also used for thermal cycling at 610˚C. It was found that the CBA increased the porosity, which resulted in the increase of the axial tensile strength reaching 3.5 MPa for sand-clay and ash ceramic. The ceramic balls with the required tensile strength for TES were selected. Their volumetric heat capacity, and thermal conductivity range respectively from 2.4075 $MJ{\cdot}m^{-3}{\cdot}{}^{\circ}C^{-1}$ to 3.426 $MJ{\cdot}m^{-3}{\cdot}{}^{\circ}C^{-1}$ and their thermal conductivity from 0.331 $Wm^{-1}{\cdot}K^{-1}$, to 1.014 $Wm^{-1}{\cdot}K^{-1}$ depending on sand origin, size and firing temperature. The selected formulas have good thermal stability because the most fragile specimens after 60 thermal cycles did not present any cracks. These properties allow envisioning the use of the ceramic balls developed as filler material for thermocline thermal energy storage (structured beds) in Concentrating Solar Power plants. And for other applications like solar cooker and solar dryer.

Keywords

Ceramic Ball, Sand, Clay, Coal Bottom Ash, Thermal Energy Storage Material, Thermocline, Concentrating Solar Power Plant

1. Introduction

The global demand for energy is growing and conventional resources like coal and petroleum are depleting; renewable resources are expected to play a crucial role in the future. In addition, the average electricity rate access in Sub-Saharan countries is very low (32%) [1], and this rate is more critical in rural area where more than 70% of the population lives on electricity rate of 17%. However, this part of Africa has a huge potential in renewable energy (PV, wind turbine and CSP) that could help increase access to energy. Apart from PV and wind turbine plant, CSP is not well known in this region of Africa. While, the region has a long hour of sunshine, with significant DNI (exceeding 5.5 $kWh \cdot m^{-2} \cdot day^{-1}$) [2] and good CSP potential (21.3 GW for parabolic trough technology) [3]. This may be explained by the CSP technology affordability suffering from energy storage system for electricity dispatching during the night-time or cloud cover. Since the current storage system increase the initial investment from 15% to 20% due to the two-tank storage system and the high price of heat transfer fluid (HTF) and storage materials like mineral oil and synthetic oil [4]. The challenge of mineral oil is the high risk of flammability, for example, in 2009 the solar field of Andasol CSP plant in Spain took fire [5]. To face these challenges in 2004 an engineering study showed the possible reduction of 10% of levelized electricity cost using molten salt in the medium storage [4] became the most effective thermal energy storage material, used in a most CSP plant, like *Andasol*, *Ouarzazate*, which is of molten salt has storage material medium [6] [7]. **Figure 1** presents the conventional two tank use in CSP for thermal energy storage. The two thank storage system can either be a direct or indirect storage system. Direct storage applies when the HTF is directly in contact with the storage medium, which circulates through the collector field. And when the storage medium is separate and keeps the tank to be in a molten salt state [8], the storage is indirect.

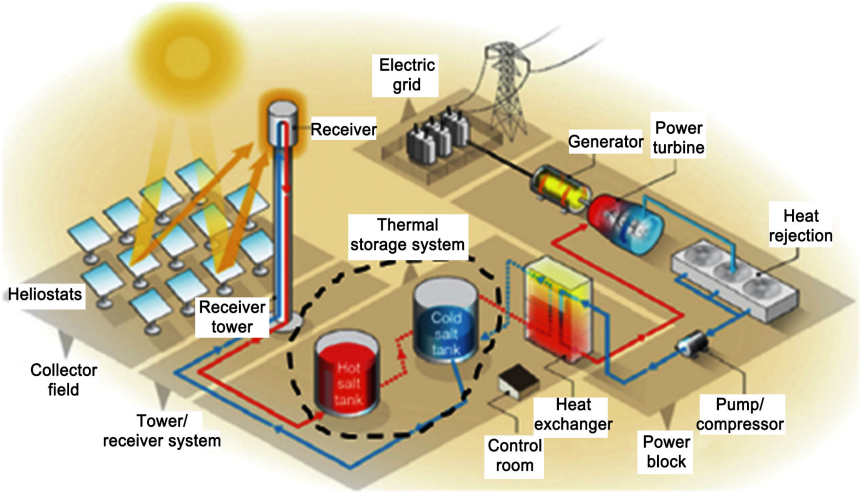

Figure 1. A state-of-the-art power tower second generation CSP plant with two tank molten nitrate salts as TES/HTF materials [9].

Despite the success of a two tank thermal storage system, there is some demerit. 1) The system is not cost-effective because there need for an extra heat exchanger which may increase the storage system cost; 2) The molten salt is also compromised due to its high melting temperature (>100˚C) and managing its thermal stability could be tedious and complex [5] [10]. 3) In addition, the use of these materials has negative impact on the environment. Although, studies have shown that there is a possibility to have a broad reduction of CSP cost from 33% to about 35% by removing one of the storage tank system which has made the storage system non-economically. To improve on the system, thus enabling the use of a single tank system instead of two, the use of eco-materials such as natural rocks, industrial waste, concrete, ceramic, etc. as filler materials [6] [11] [12] [13] inside one tank calls thermocline tank as illustrated in **Figure 2**. The thermocline storage can also be direct or indirect as discussed previously for two tanks system.

Several filler materials' potentials were discussed in [14]-[23]. Eco-materials such as Rhyolite and Quarzitic sandstone with good thermal capacity of around 2800 $kJ \cdot m^{-3} \cdot K^{-1}$ and 2250 $kJ \cdot m^{-3} \cdot K^{-1}$ respectively at 600˚C are likely to be the most effective eco-material for typical thermocline tank [24]. However, a main demerit is that such eco-material could possess low sphericity and irregular size (big size) which may reduce the thermal storage efficiency as discussed in [25]. To achieve more effective storage efficiency as reviewed in [26], the thermocline should be thin, and an optimum thickness would be achieved with particle dimeter less than 3 cm. This optimum point reached was as result of the heat transfer process that existed between the heat transfer fluid and the particle surface, which depends on the particle size [25] [27]. In order to overcome challenges due to shape and size, material formulation is required.

Several studies have employed material formulation as a required process to overcome issues relating to shapes and sizes in heat transfer processes in raw material [28] [29] [30] More studies have employed the use of ceramics from

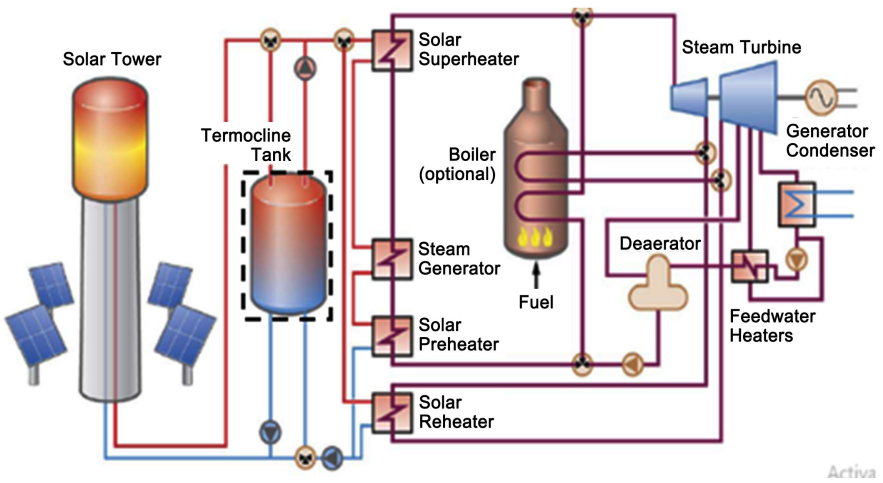

Figure 2. Single tank thermocline system [8].

clay and ash for sensible heat storing, which include: Lopez *et al.*, [31] made pressed plates ceramics from incinerator bottom ashes and waste clay using sintering method at different temperature level. Result from Lopez revealed a preferred and sustainable mechanical performance (more than 30 MPa) with thermally stable specimens, however, the volumetric specific heat capacities were limited. Similarly, based on X-ray pair distribution function analysis, differential scanning calorimetry according to Nigay *et al.* have shown the possibility of achieving more than 1.49 $kJ \cdot kg^{-1} \cdot K^{-1}$ as specific heat capacity with flexural strength of 11.1 MPa for ceramic made with clay and 30 wt% of biochar using sintering method up to 950˚C [21]. Sane *et al.*, buttressed this by showing that the clay ceramic thermal conductivity can increase with the wt% of silicon-carbide [20].

By mixing slaked lime with bottom ash or laterite from Burkina and Niger, Kenda *et al.*, have developed ceramic by melting the raw materials with concentrating solar technology. These ceramics were estimated to have good thermal properties and cost-effective than industrial ceramics [28]. From the literature, we can conclude that the specific heat capacity of most ceramic range between 700 and 1490 $J \cdot kg^{-1} \cdot K^{-1}$.

Thermal energy storage material (TESM) should have a compressive strength higher than 1 MPa, ability to withstand thermal cycling, high volumetric heat capacity [14] and thermal conductivity higher than 1 $Wm^{-1} \cdot K^{-1}$ is desirable [32]. However, the effect of thermal conductivity could be negligible on thermocline energy storage performance [33]. Sands (dune, river and mining sand) have potentiality to be use as sensible heat storage materials [34] [35] but have issues of agglomeration at high temperature. Hence, to face these challenges, the main objective of this work is to use sand, clay and coal bottom ash (CBA) More so, issues relative to particle shape and cost, availability, environmental performance have motivated research and development (R&D) efforts to develop recycled ceramics made of locally and naturally available materials. Hence, this study aims to solve these challenges through the use of sand, clay and coal bottom ash (CBA) locally available, obtained from different regions of West Africa to develop an effective TESM. The study's specific objective includes: 1) different ceramics will be shaped by mixing different percentage weight (wt%) of sand, clay and CBA. 2) to study and present the best ceramics, the thermos-mechanical properties and thermal stability of each ceramic as a good source of sensible thermal energy storage.

2. Material and Method

2.1. Material Formulation Process

2.1.1. Raw Materials

West Africa has a huge potential for raw material resources that could be used to formulate thermal energy storage material, and this was explicitly investigated in [28] and in our previous work [36]. In the present work sand, clay and coal bottom ash (CBA) from a different region in West Africa (Burkina and Niger) are

mined and used to formulate ceramic for sensible heat storage. The main mineral composition of sands studied in Burkina Faso and Niger is up to 80% of quartz (SiO_2), 9% of Alumina (Al_2O_3) and some other oxide [37] [38]. Clay is an argillaceous material usually composed of complex natural mixtures of minerals presenting very variable grain size and physicochemical properties. Clay is an argillaceous material usually composed of complex natural mixtures of minerals presenting very variable granulometry and physicochemical properties [39]. The different clays studied in Burkina Faso contain mainly kaolinite (>40 wt%), illite (>13 wt%), quartz (>18 wt%) and rutile (1 wt%) [39]. The chemical composition of the CBA used is reported in **Table 1** and size distribution of dune and mining sand is reported in [26] [40].

2.1.2. Raw Materials and Sampling Sites

In addition to the sand study in our previous work [42], two other samples were collected in Niger. The dune sand was collected around Agadez (16.966686˚N, 7.9833353˚E) and the natural sand around Ingall (16.7855571˚N, 7.9322241˚E). For the clay samples, one was collected from the deposit of Malgsombo (12.4527288˚N, 1.4050814˚E) in the commune of Saaba (C) and the second one from the deposit of Ethouayou (12.0587723˚N, −3.03435˚E) in the commune of Tcheriba (C1). The main difference between the both, is the colour (brown (C) and green (C1)), also in terms of use, the first one is used to make brick or fired brick for building and the second one is used to make pottery also by firing. Both of them have been obtained by digging. The CBA was collected directly from the incinerator bottom of Niger State company (SONICHAR) coal power plant instead of the landfill where more than 2 million tons are already available and 150,000 tons are wasted there every year [28].

2.1.3. Materials Processing Method

1) Sifting and milling

A sieve of 1 mm was used to sift the different sand samples. This operation was not necessary for dune sands due to their small (<0.3 mm). The clay samples (binder) were sifted with sieve of 0.5 mm after milling them with a porcelain miller. About 7 kg of the CBA sample was milled for about 10 minutes into powered form in an electrical miller and used directly for the formulation. The different samples after treatments are presented in **Figure 3**.

2) Formulation description

a) Thermal energy storage material (TESM) shaping

Shaping the filler materials is important for thermocline storage systems. A spherical shape is required to achieve better contact between the heat transfer fluid and the filler material. In this work, a mould with six spherical elements of 3cm diameter was designed and made locally to shape the material. During the formulation, firstly, the mass of clay (binder) was weighted to be equal to the porosity of the sand. The porosities of the sand samples were assumed to be 42% for mining sand from Burkina and natural and dune sand from Niger and 45 wt% for dune sand from Burkina [36] [40]. The formulas were obtained with 58 wt%

Table 1. Chemical compound of Coal bottom ash [28] [41].

Composition (wt%)	SiO_2	Fe_2O_3	Al_2O_3	MgO	TiO_2	CaO	K_2O	LOI
CBA	35.63 - 62.12	3.93 - 5.58	19.43 - 27.13	1.24	2.62	0 - 0.5	2.05	15

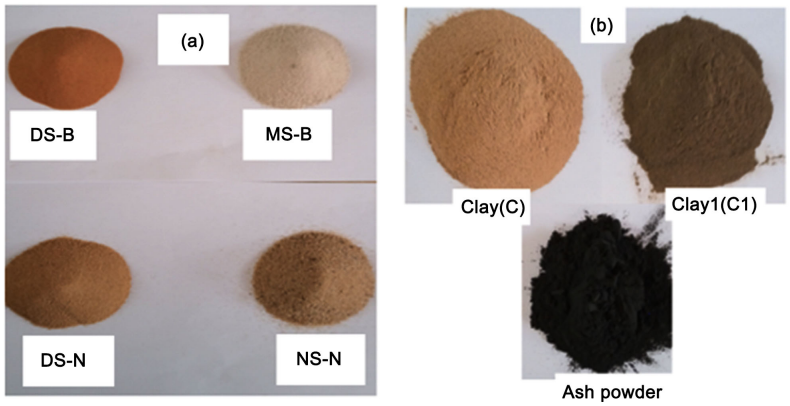

Figure 3. Raw materials: (a) Dune sand from Burkina (DS-B), mining sand from Burkina (MS-B), dune sand from Niger (DS-N), natural sand from Niger (NS-N); (b) clay from Malgsombo deposit (C), clay from Ethouayou deposit (C1), CBA powder).

or 55 wt% of sand and 42 wt% or 45 wt% of clay. For the second formulation, 12 wt% of clay ratio was replaced by ash to know the effect of the ash on the ceramic mechanical performance. The composition of these formulas becomes 58 wt% or 55 wt% of sand, 12 wt% of bottom ash and 30 wt% or 33 wt% of clay. Finally, the ratio of the ash was increased to 30 wt% to obtain pellets with 40 wt% of sand, 30 wt% clay and 30 wt% of ash. Water was mixed and each element of the mould was pressed with human force. The clay fraction is supposed to provide the shape by providing plasticity and dry mechanical strength during processing. During firing, clay and kaolinite have a role in mulita recrystallization and in the formation of a vitreous phase. Feldspars contribute in the quantity and behaviour of the liquid phase at temperatures above 1050˚C [39] [43]. **Table 2** presents an example of some formulations with their nomenclatures.

Each formulation was replicated at least six times to check the reproducibility of experimental results. The same formulation was done and replicated with clay C1.

b) Drying and sintering process

After shaping the different specimens were dried at 105˚C in an oven during 24 hours to remove all water from the specimens. Then, the weighted specimens (m_0) were put within a muffle furnace and fired with heat rate of 3˚C from room temperature to 500˚C, 2˚C heating rate from 500˚C to 1000˚C and held at 1000˚C for 4 hours after being cold down to 50˚C with cooling rate of 2˚C. The same process (**Figure 4**) was repeated for the pellets obtained at 1060˚C. After firing the specimens were weighted (m_1) and the loss on ignition was computed using the following equation.

$$\mathrm{LOI} = \frac{m_0 - m_1}{m_0} \times 100 \quad (1)$$

Table 2. Different weight of raw materials and water used for ceramic balls formulation.

Formulas	Sand weight (g)	Clay weight (g)	Ash weight (g)	Water weight (g)	M_{water}/m_{binder}
D55C45-B	99	81	0	19.5	0.24074074
D55A12C33-B	99	59.4	21.6	23.9	0.29506173
D40A30C30-B	72	54	54	25.8	0.23888889
M58C42-B	104.6	75.6	0	23.3	0.30820106
M58A12C30-B	104.4	54	21.6	22.5	0.29761905
M40A30C30-B	72	54	54	27.8	0.25740741
D58C42-N	104.4	75.6	0	21.2	0.28042328
D58A12C30-N	104.4	54	21.6	20.5	0.27116402
D40A30C30-N	104.4	54	21.6	24.1	0.31878307
N58C42-N	104.4	75.6	0	19.1	0.2526455
N58A12C30-N	104.4	54	21.6	21.9	0.28968254
N40A30C30-N	72	54	54	25	0.23148148

Figure 4. Drying and firing process.

2.2. Characterization of the Sintered Materials

2.2.1. Mechanical Properties

1) Bulk density and porosity

To store thermal energy, the filler materials' density, plays a crucial role because it influences TES capacity. High is the density, high is the volumetric heat capacity. It is important input data for sensible heat storage system modelling [44]. So, the apparent density of the different specimens (ceramic balls) was measure using Archimedes' method. This method is useful to determine the bulk and apparent density of any regular or irregular material, including ceramic. The test specimens were dried out at 105˚C for 12 hours to ensure total water loss. Their dry weights were measured in air in suspended condition and recorded. They were allowed to cool and then immersed in a beaker of water. Bubbles were observed as the pores in the specimens were filled with water. Their soaked weights were measured in air and in water in suspended condition and recorded. The soaked weights were measured also after 15 hours in water in suspended condition to compute the porosity. Bulk density and porosity of the samples were calculated using the equations below:

$$\rho_b = \frac{m_{\text{dry in air}}}{m_{\text{soacked in air}} - m_{\text{soacked in water}}} \times \rho_w \quad (2)$$

$$\varepsilon = \frac{m_{\text{soacked in air}} - m_{\text{dry in air}}}{m_{m_{\text{soacked in air}} - m_{\text{soacked in water}}}} \times 100 \tag{3}$$

2) Mechanical strength

Determination of mechanical strength is not an easy thing, especially when the size of the specimen is small and the shape is spherical. In the literature, several models are proposed for irregular and spherical material mechanical strength determination. Based on the value of tensile strength obtained by the Brazilian test with flat platens (plaster of Paris, coal and cement) [45], JAEGER, developed a model to compute the tensile strength of four spherical rocks as follows [46]:

$$\sigma_t = k\frac{F_f}{R^2} \tag{4}$$

where K is a numerical constant, F_f the peak load at failure of the sphere and R the radius of the sphere.

The following year in 1967 HIRAMATSUS and OKA determined the tensile strength of rock by a compression test of an irregular test piece. They showed that the theoretical peak tensile is considerably greater than below validated equation with experimental results [47]:

$$\sigma_t = 1.4\frac{F_f}{\pi R^2} \tag{5}$$

Many experimental studies have used these expressions to evaluate the strength of spherical or irregular particles tested in uniaxial compression [47] [48] [49].

In this study the quasi-static method was used. Uniaxial compression test, in which a particle is compressed between two parallel platens of a compression machine until it fails. The peak load was recorded during the test, then the axial tensile strengths were computed for 3 specimens for each formulation using the Equation (6) with $k = 1.4$ as done in [47]. The sand-clay and CBA ceramic balls were tested as showed in **Figure 5**.

For the different mechanical properties, the standard errors were computed using the following equation:

$$\text{SE} = \frac{\sqrt{\sum\left(x_i - \bar{x}\right)^2}}{\bar{x} \times n} \times 100 \tag{6}$$

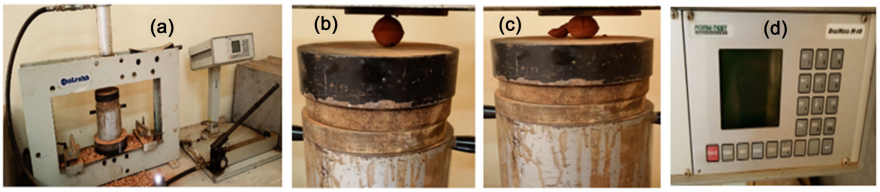

Figure 5. Compression test process: (a) compression machine, (b) insertion of specimen between the two parallel platens, (c) fail of the specimen under the maximal load and (d) the display screen.

The maximum standard errors or uncertainties obtained for the different mechanical properties are 6%, 2.94%, 4.91% and 10% respectively for the bulk density, porosity, loss on ignition and axial tensile strength according to the formulation.

2.2.2. Thermal Properties

Portable, battery-operated KD2 Pro Thermal Properties Analyser with dual needle sensor was used to measure volumetric specific heat capacity, thermal conductivity and thermal diffusivity. The dual-needle SH-1 sensor (1.3 mm diameter 30 mm long for a needle) was chosen to perform the tests as the producer recommends [50] it for porous material and other material like granular material (soil, sand) and rocks. Pilot hole was drilled using a drilling machine with a drill bit of 1 mm and 1.5 mm. Measuring range is 0.5 to 4 $MJ{\cdot}m^{-3}{\cdot}K^{-1}$ for volumetric heat 0.02 to 2 $W{\cdot}m^{-1}{\cdot}K^{-1}$ for thermal conductivity and 0.1 to 1 $mm^{2}{\cdot}s^{-1}$ for thermal diffusivity with accuracy of ±10% for the sensor. The dual sensor calibration specimen was used to calibrate the sensor before any test. The read time was chosen to minimise the error in the results (<0.01) and the measurements were replicated at least three times on two different pellets of the same formulation.

2.2.3. Thermal Stability Analysis

An average CSP plant is expected to last at least 10 - 30 years, which could require thousands charge-discharge cycles [14] [24] [29]. To reduce the number of cycles performed for each sample, the rate of heating and cooling was increased during the charge-discharge cycles. When the ceramic balls will have thermal stability at high heating rate, their thermal properties will be even better for low heating rates [24] (In the storage system). The thermal cycles were carried out in a programmable muffle furnace at 610˚C with a heating rate of 20˚C/min (less than 1˚C/min in normal operation), the temperature was held during one hour at 610˚C and a discharge cycle was carried out at ambient air to 100˚C for thirty-three minutes with a cooling rate of 14˚C/min. A multimeter with thermocouple was used to control cooling rate by tracking the time. The thermal stability study process is presented in **Figure 6**. After the 60 cycles, the specimens were weighted for mass loss appreciation. The examined ceramic balls have a similar mean diameter of around 2.88 cm.

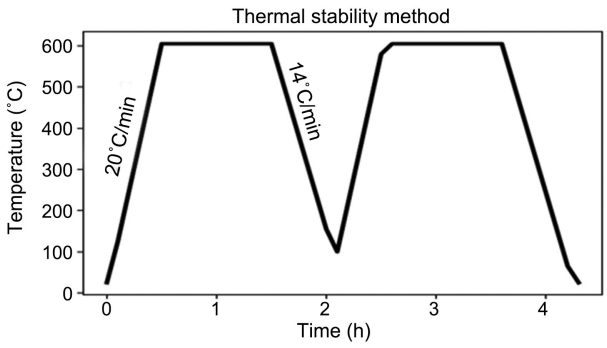

Figure 6. Thermal stability study method.

2.2.4. Selection Method

Keeping in mind the criteria established by the IEA, the formulated material must meet certain requirements to be used as TESM in solar power plants. The filler material needs to have sufficiently high compressive strength so that the bottom layer does not crush under the load of the ceramic ball piled above it. For a packed bed 25 m high, the average load at the bottom would be below 1 MPa for a particle density of 3000 $kg{\cdot}m^{-3}$ [14]. For any formulated or filer material (ceramic or rocks) that weathers rapidly and forms dust or sand (disintegrates) that fills the heat transfer fluid passages in the bed is undesirable [14]. The filler material must have a** high storage capacity (ρc_p > 2 $MJ{\cdot}m^{-3}{\cdot}K^{-1}$) to reduce the volume of thermal storage tank and this will result in lower material costs, but also lower tank costs. The thermal conductivity needs to be sufficiently high to allow the heat to be conducted from the outer surface of the particle to the core with a small temperature gradient through the particle. In this study the first step of selection was based on the analysis of axial tensile strength of the ceramic ball, the second step the analysis of the thermal properties and the last step was based on the thermal stability analysis. The selection of SHS materials based on thermal cycling is not yet standardized. In 2019 Sane *et al.*, after 20 cycles at 700˚C under air atmosphere with 5˚C/min as heating rate and based on mass losses observation came out with appropriate ceramic for TES made with clay and 20 wt% SiC (silicate carbide) [20]. Base on crack observation and mass loss Allen *et al.*, in 2014 have shown that rock like igneous and high-grade metamorphic is suited for sensible heat storage (SHS) application after 950 cycles at mean temperature of 350˚C and 500˚C - 530˚C with heating rate of 2˚C/min [14]. In 2017 Tiskatine *et al.*, have demonstrated the SHS suitability of quarzitic base on crack observation after 120 thermal cycles at 650˚C under air atmosphere with heating rate of 25˚C, 1h isotherm and cooling rate of 20˚C [24]. After three cycles at 1000˚C with heating rate of 10˚C /min and in a TMA/TG-ATD devise, Ferber *et al.*, have come out with suitable SHSM ceramic made with 20 wt% and 30 wt% clay and Municipal Waste Incineration Bottom Ash (MWIBA) [51].

3. Results and Discussion

3.1. Mechanical Properties Analysis

Figures 7(a)-(c) and **Figures 8(a)-(c)**, present the results (illustrated cases) of the bulk density and axial tensile strength for each formulation respectively at 1000˚C and 1060˚C.

The bulk density values range from 1730 kg/m^3 to 2050 kg/m^3 (±6%) and are similar to the one developed in the literature [52]. The overall bulk density of the pellet decreased with the increase of CBA ratio and the decrease of sand ration except the one obtained with the NS-N and C1 at 1060˚C. For example, it decreases by 9.71%, 6.21%, 1.12%, and 7.82% respectively for dune and mining sand from Burkina and dune sand and natural sand from Niger for the pellet fired at 1000˚C. The volatile elements, which influence the LOI in the different

sand can explain the difference in decrease ratio especially for MS-B, DS-N and NS-N. This decrease could also be explained by the reduction of sand ratio because clay-sand ceramic density increase with fine sand ratio [52].

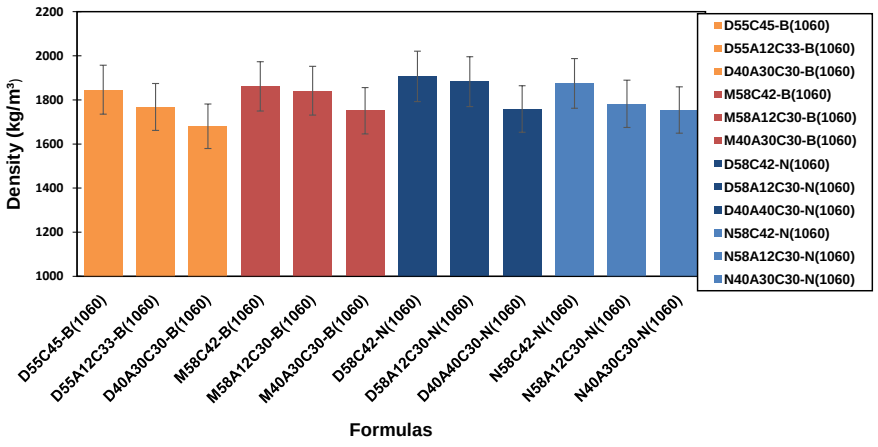

(a)

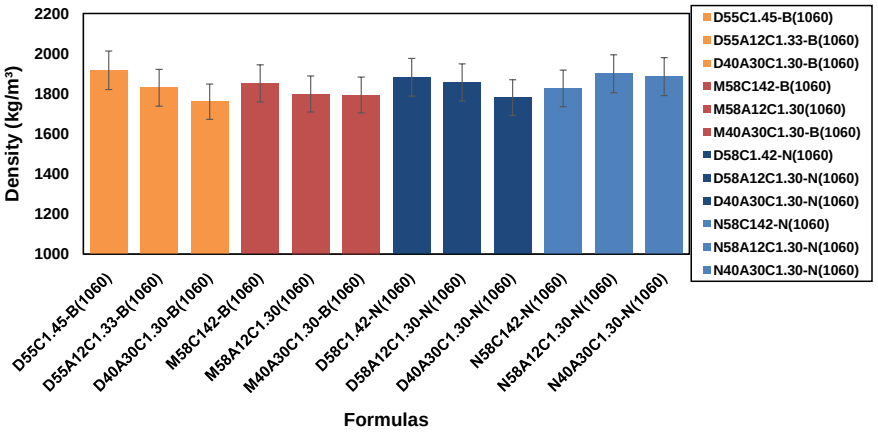

(b)

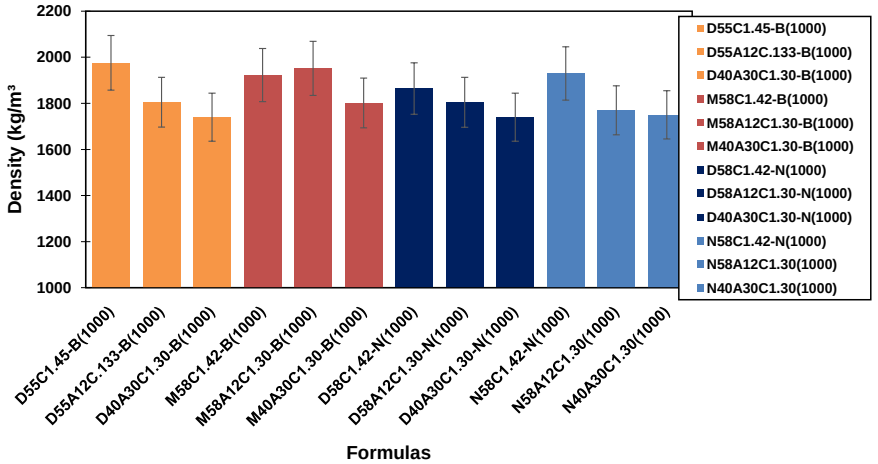

(c)

Figure 7. Bulk density of some specimens formulated with the different sand CBA and clay (C1) at 1000˚C (a) and at 1060˚C (b) and with clay (C) at 1060˚C (c).

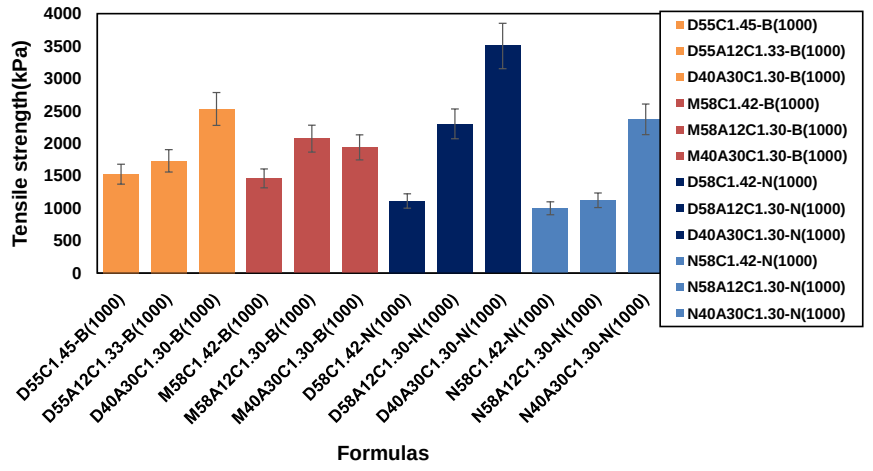

(a)

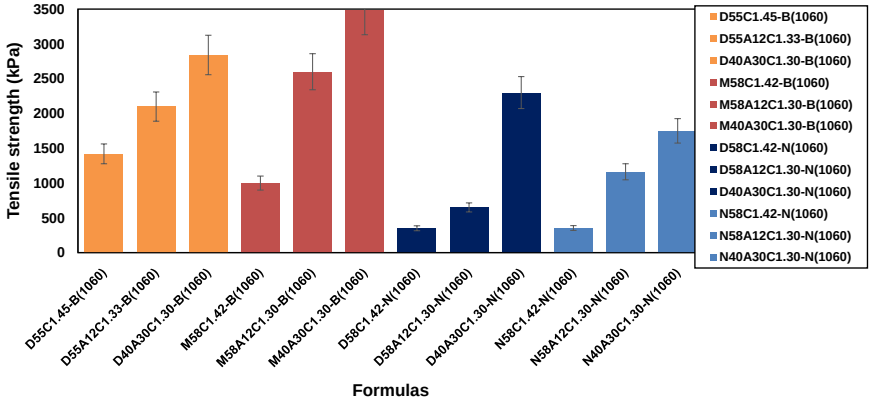

(b)

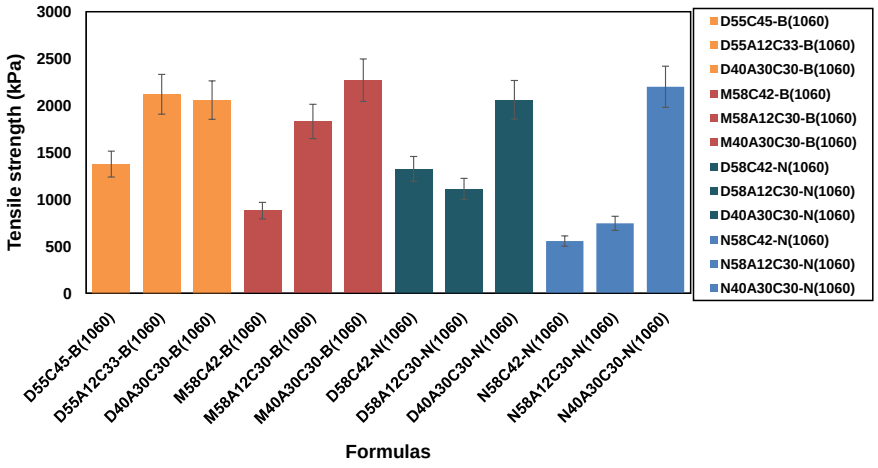

(c)

Figure 8. Uniaxial tensile strength of the different specimens formulated with the different sand, CBA and clay (C1) at 1000˚C (a) and at 1060˚C (b) and clay (C) at 1060˚C (c).

The porosity and LOI results during the formulation of the different ceramic balls range respectively from 20.8% to 28.57% (±2.94%) and 2.08 wt% to 5.71 wt% (±4.91%) according to the formulas.

The results show a slight decrease of the bulk density with increasing CBA wt% as illustrated in **Figure 7**. The increase of the porosity with CBA ratio could justify the decrease of the density due to the increase of mass loss, which increases the void volume. The trend of bulk density as function of porosity is illustrated in **Figure 9**. As the loss on ignition of CBA is high (15%), increasing its mass will drive to the increase of the specimens' loss on ignition during firing which will increase the porosity of the specimen as illustrated in **Figure 10**.

For the axial tensile strength their values ranged from 350 kPa to 3500 kPa with standard error of ±10% according to the formulation. The results are presented in **Figures 8(a)-(c)**. An improvement with the CBA ratio in all the formulation (ceramic ball) has been observed. The results are similar to the flexure strength obtained by [52] with sand-clay ceramic. The objective of this study being to combine sand particles together to improve it thermal properties of TESM, the tensile strength of the gotten ceramics is acceptable for all balls ceramic which contain ash waste, excepted N58A12C30-N and N58A12C1.30-N. The increase of CBA ratio in sand and clay ceramic shows an improvement of the axial tensile strength while the porosity increases. This shows that the ash plays a rule of binder like clay. Despite the fact that, the porosity of the specimen increase with CBA wt%, an increase of the tensile strength is observed (**Figure 11**). This can be explained by the chemical composition of the CBA given in [28] and the other raw material (clay and sand). Generally, raw materials for ceramic pastes containing $CaCO_3$ are liable to form crystalline phases at relatively low temperatures from 950˚C to 1000˚C [53]. In addition, alkaline contributes to the formation of liquid phases at low temperatures [54]. As the ratio of alumina (Al_2O_3) is enough in the CBA, it could contribute to an increase the quantity of kaolinite. Therefore, during heat treatment, the major component of kaolinite is transformed into metakaolinite between 550˚C to 600˚C, with a dehydrated metastable amorphous structure. Between 950˚C to 1000˚C, it is very progressively transformed into an alumina spinel phase and amorphous silica. Just above 1000˚C, feldspar grains react with the amorphous silica and metakaolinite to form a viscous liquid. This process involves the progressive dissolution of the finest quartz grains into the liquid phase [39] [55]. The last process might be limited during the firing of the present ceramic (more limited for natural sand with 0.93 mm mean grain size), because the maximum firing temperature was 1060˚C while larger quartz (main component of the raw materials) grains dissolution begins at temperature up to 1100˚C [39] [55]. That can explain the high porosity of the specimens because the dissolution of quartz drives the reduction of ceramic pores. These phenomena could be the difference from one clay to another because the highest tensile strength ceramics have abstained with pottery clays (CI). In the end, we can conclude that CBA was successfully integrated with a ceramic formulation, potentially providing an end-use for this waste at a temperature less than 1100˚C.

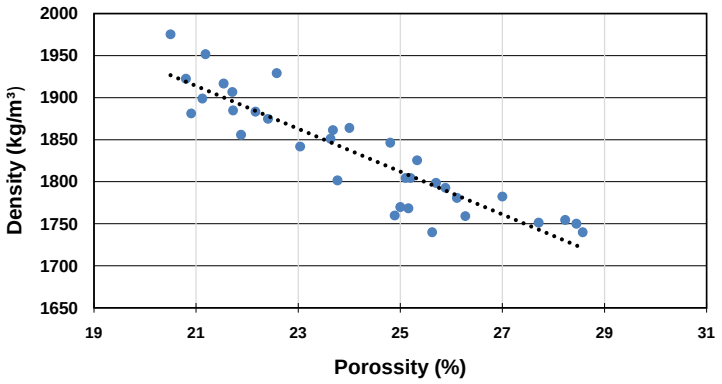

Figure 9. Effect of porosity or ash percentage weight on the ceramic balls bulk density.

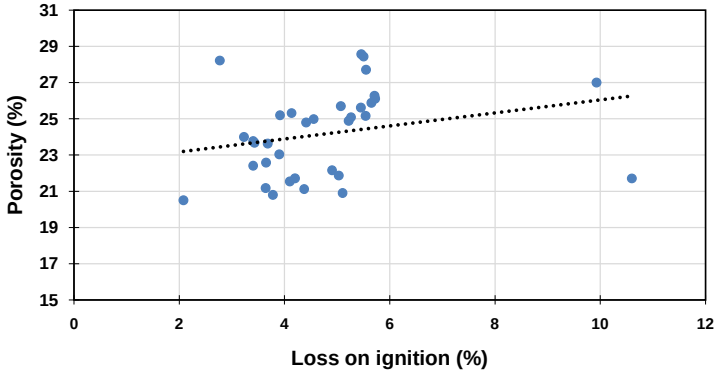

Figure 10. Effect of CBA wt% increasing on the porosity and the loss on ignition of some specimen.

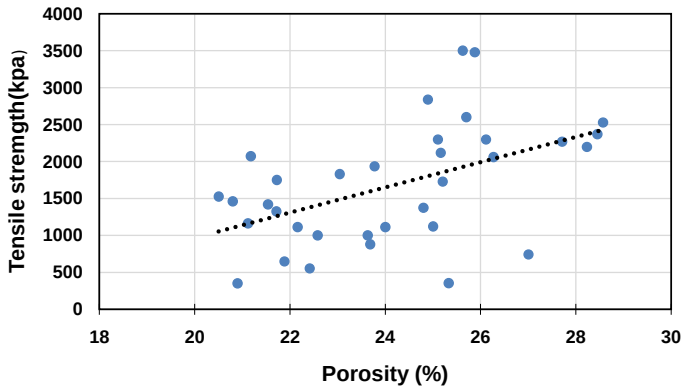

Figure 11. Effect of porosity or ash percentage weight on the ceramic balls tensile strength.

However, to select the best TESM base on the tensile strength, it is better to take into account the compressive strength dropped during heat treatment. This drop of compression strength can reach 30% to 60% for rocks like granite depending on the working temperature [56]. To avoid any ball crushes in the storage system, a minimum compression strength of 1MPa is needed. However, this drop of mechanical performance could be low for ceramic or porcelain speci-

mens due to their refractory character defined as the collapse of the material under its own weight at high temperatures [57]. Therefore the ceramic balls formulated with sand, clay and CBA excepted N58A12C30-N and N58A12C130-N have been considered in the following work for thermal analysis.

3.2. Thermal Properties Analysis

The overall ceramic balls developed with sand clay and CBA excepted the formulations N58A12C30-N(1060) and N58A12C120-N(1060) have been selected based on the mechanical strength performance. Their thermal properties have been assessed with accuracy of ±10% and measurement error, and presented as Table 3 and Table 4 with the different standard errors.

Table 3. Thermal properties of the ceramic balls sintered at 1000˚C.

Formulation	λ ($Wm^{-1}\cdot{}^{\circ}C^{-1}$)	D ($mm^2\cdot s^{-1}$)	ρc_p ($MJ\cdot m^{-3}\cdot{}^{\circ}C^{-1}$ J)	Temp (˚C)
D55A12C1.33-B(1000)	0.397 (±1.63%)	0.1565 (±1.27%)	2.539 (±2.21%)	30.8 (±5%)
D40A30C1.30-B(1000)	0.3665 (±3.2%)	0.134 (±1.63%)	2.7365 (±1.63%)	31.885 (±0.77%)
M58A12C1.30-B(1000)	1.014 (±0.28%)	0.135 (±0.165%)	2,906 (±0.19%)	31.48 (±1.86%)
M40A30C1.30-B(1000)	0.383 (±3.2%)	0.13733333 (±0.4%)	2,789 (±0.84%)	26.41 (±0.34%)
D58A12C1.30-N(1000)	0.382 (±3.67%)	0.152 (±3.72%)	2,624 (±8.2%)	34.12 (±9%)
D40A30C1.30-N(1000)	0.373 (±0.15%)	0.148 (±0.38%)	2.513 (±0.20%)	30.51 (±2.58%)
N40A30C1.30-N(1000)	0.407 (±2.06%)	0.164 (±1.405%)	2.476 (±3.476%)	31.073 (±5.17%)

Table 4. Thermal properties of the different ceramic ball sintered at 1060˚C.

Formulation	λ ($Wm^{-1}\cdot{}^{\circ}C^{-1}$)	D ($mm^2\cdot s^{-1}$)	ρc_p ($MJ\cdot m^{-3}\cdot{}^{\circ}C^{-1}$ J)	Temp (˚C)
D55A12C1.33-B(1060)	0.456 (±0.33%)	0.177 (±3.72%)	2.596 (±1.32%)	34.62 (±2.71%)
D40A30C1.30-B(1060)	0.411 (±0%)	0.173 (±4.08%)	2.4075 (±5.72%)	29.76 (±2.18%)
M58A12C1.30-B(1060)	0.4185 (±0.5%)	0.167 (±1.27%)	2.5095 (±1.54%)	36.55 (±2.47%)
M40A30C1.30-B(1060)	0.47 (±0.12%)	0.174 (±0.57%)	2.70 (±0.7%)	24.7833333 (±1.46%)
D58A12C1.30-N(1060)	0.416 (±0%)	0.155 (±1.5%)	2.693 (±1.39%)	27.2566667 (±6.16%)
D40A30C1.30-N(1060)	0.414 (±1.53%)	0.148 (±3.59%)	2.798 (±2.53%)	35.5 (±4.93%)
N40A30C30-N(1060)	0.41 (±0.54%)	0.138 (±0.36%)	2.971 (±0.18%)	27.92 (±10%)
D55A12C33-B(1060)	0.371 (±0.38%)	0.121 (±0%)	3.0545 (±0.44%)	32.17 (±0.13%)
D40A30C30-B(1060)	0.4025 (±0.2%)	0.135 (±0%)	2.5515 (±0.47%)	29.37 (±7.8%)
M58A12C30-B(1060)	0.473 (±0.32%)	0.138 (±2.17%)	3.426 (±1.51%)	30.505 (±3.58%)
M40A30C30-B(1060)	0.436 (±0%)	0.167 (±0.32%)	2.612 (±0%)	27.065 (±0.16%)
D58A12C30-N(1060)	0.42 (±0%)	0.15825 (±0%)	2.7765 (±0.076%)	30.9375 (±0.38%)
D40A30C30-N(1060)	0.331 (±7.4%)	0.123 (±6.19%)	2.713 (±4.34%)	34.78 (±5.1%)
N40A30C30-N(1060)	0.411 (±0.24%)	0.141 (±0.82%)	2.916 (±1.15%)	25.66 (±7.28%)

The thermal conductivity of the different specimens ranges from 0.331 $Wm^{-1}\cdot K^{-1}$ to 1.014 $Wm^{-1}\cdot K^{-1}$ with standard error of less than 10% for each formulation. In general, the thermal conductivity obtained is less than the required value need for a thermal energy storage material (≥1 $Wm^{-1}\cdot K^{-1}$) except the formulation M58A12C1.30-B(1000). The overall thermal conductivity is low for the pellets. The effect of CBA ratio and firing temperature is not significate on thermal conductivity. However, the minimum thermal conductivity is 0.331 $W\cdot m^{-1}\cdot K^{-1}$ showing that sand and ash improve the thermal conductivity of the different ceramic balls developed and can even reach 1.014 $Wm^{-1}\cdot K^{-1}$, compared to clay ceramic thermal conductivity obtained without any additive fired at 1200˚C in [52] which is around 0.3 $Wm^{-1}\cdot K^{-1}$. Below 1050˚C, the clay ceramic is not properly fired, which strongly reduced its thermal conductivity as demonstrated in [58] where a value less than 0.3 $Wm^{-1}\cdot K^{-1}$ was measured for kaolin clay ceramic fired at 1050˚C. As the effect of thermal conductivity on TES performance can be negligible [33], the obtained ceramic balls could stand well in term of conduction characteristic.

The thermal diffusivity of the different pellets ranges from 0.123 $mm^2\cdot s^{-1}$ to 0.177 $mm^2\cdot s^{-1}$ with standard error less 10% for each formulation. As the thermal diffusivity is the ratio of thermal conductivity to volumetric heat capacity, it can be defined as the rate of temperature spread through a material and measured the heat transfer from the hot material to the cold. A high value of thermal diffusivity can drive to the degradation of thermocline energy storage by thermal diffusion [59]. In the literature, a required thermal diffusivity value for thermal energy storage is not available, however, a reasonable thermal diffusivity is required to avoid thermocline degradation.

The volumetric heat capacity or volumetric specific heat (VHC) of the different ceramic balls ranges from 2.4075 $MJ\cdot m^{-3}\cdot ^\circ C^{-1}$ to 3.426 $MJ\cdot m^{-3}\cdot ^\circ C^{-1}$ with standard error less 10% for each formulation as presented in **Table 1** and **Table 2**. The results are better for the composition with 58 wt% or 55 wt% sand, 12 wt% ash and 33 wt% or 30 wt% clay because the highest VHC is obtained with M58A12C30-B(1060). This can be explained by the sand particle size effect on the specific heat capacity which is around 0.26 mm, 0.91 mm and 0.93 mm respectively for dune sand, mining sand and natural sand. Increasing and reduction respectively of the ash powder wt% and sand wt% could drive to the reduction of the mean particle size in the ceramic. As consequence, the volumetric heat capacity can drop as demonstrated by Bwayo *et al.*, in 2014 on specific heat capacity which increases with particle size (sawdust) of fired brick developed from sawdust and clay [60]. However, all the ceramic ball developed in this study met the required VHC (up to 2 $MJ\cdot m^{-3}\cdot ^\circ C^{-1}$) to be used as sensible heat storage materials in the CSP plant according to Fernandez *et al.*, [32]. Some ceramic balls have a volumetric heat capacity higher than 3 $MJ\cdot m^{-3}\cdot ^\circ C^{-1}$ at room temperature (**Table 3** and **Table 4**) and can become better at high temperature. Therefore, the ceramics developed could compete with molten salt at high tem-

perature because the favoured molten nitrate salt has a volumetric heat capacity of 3 $MJ \cdot m^{-3} \cdot K^{-1}$, and limited to a temperature change at approximately 300˚C [61].

3.3. Thermal Stability Analysis

The thermal stability qualifies the sample loss of mass with temperature or under heat treatment. A material with high thermal stability shows high resistance to thermal decomposition. Forty-two (42) ceramic balls (numbered from 1 to 42 before the test) have been treated during 60 cycles as demonstrated in **Figure 8** including those with low tensile strength like numbers 1, 4, 6, 7, 10, 17, 20, 21, 23, 26, 29, 32, 35, 38 made only with sand and clay. After every 20 cycles, the specimens were photographed and presented in **Figure 12** as follows.

Only a colour change has been observed for all the different ceramic balls. Even the one with the lowest tensile strength did not crack after the 60 cycles. No crack has been observed after 60 thermal cycles even for the most fragile ceramic in this study. In addition, **Figure 13** present the mass loss obtained with the base of the selected specimen on tensile strength after 60 cycles. The maximum mass loss registered is 0.87% compared to 0.6% obtained by [20]. This difference can result from the raw materials type, the mechanical properties, the number of cycles which are 60 in this study again 20 and the heating and cooling rate. Therefore, we can conclude that all the ceramic balls made with sand, clay and CBA could be suited for SHS from the axial tensile strength assessment, thermal properties and thermal stability analysis.

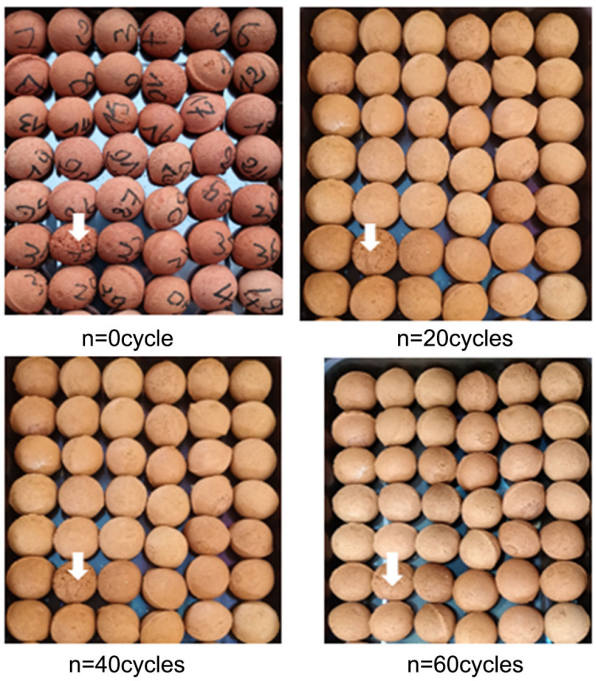

Figure 12. Photographed of the different specimens after each 20 cycles.

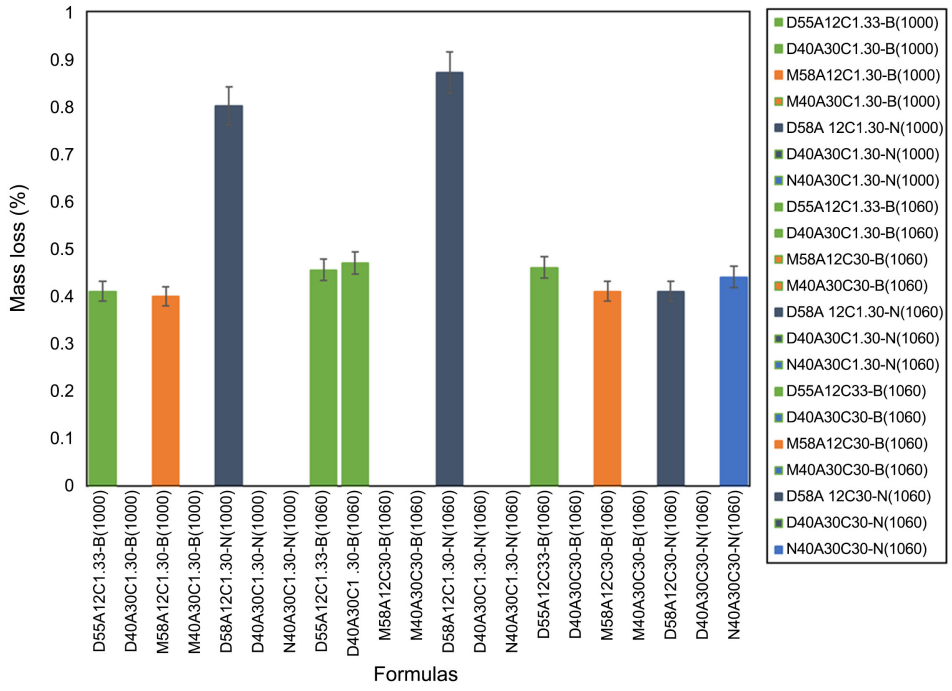

Figure 13. Mass lost by the different ceramic balls during heat treatment.

4. Conclusions

In this paper, sand particles have been combined together using clay and coal bottom ash waste from incinerator of Niger coal power plant giving a spherical shape to the material. After formulation and firing at 1000˚C and 1060˚C, the obtained ceramics were mechanically and thermally analysed. From the tensile strength analysis, the results have shown that only the formulation with ash waste has the required tensile strength for SHS except for N58A12C30(1000) and N58A12C1.30(1060) due to the large grains of natural sand. All the ceramics selected from the axial tensile strength have the required VHC for SHS and could even compete with the one of molten salt for high TES application. Based on the thermal conductivity, only the formulation M58A12C1.30-B(1000) have the required thermal conductivity. However, the thermal conductivity of the selected ceramic is close to or higher than the thermal conductivity of molten salt and thermal oil used in CSP plant. A par from that thermal conductivity has a neglected effect on TES performance. The thermal cycling showed that all the selected materials could have higher thermal stability due to the refractory character of the ceramic, the absence of crack and the low mass loss observed. This paper can be considered as thermal properties database for thermal energy storage system modelling in West Africa. Other areas of application of thermal energy storage system could be applied to chemical processes and energy systems using CSP, solar towers and solar greenhouse driers.

However, more work is needed to understand the lowest mechanical properties of the specimens made only with sand and clay and to understand the effect of the firing temperature to improve mechanical strength. In future work, the

chemical composition and mineralogy of the raw materials, the structure of the ceramic balls and their thermal properties as a function of temperature will be analysed.

Acknowledgements

This work is part of West African Science Services on Climate Change and Adapted Land use (WASCAL). Also this document was produced with the financial support of the Cuomo Foundation. The contents of this document are solely the liability of Boubou BAGRE and under no circumstances may be considered as a reflexion of the position Cuomo Foundation and/or the IPCC. The authors also thank the Laboratoire de Phyique et Chimie de l'Environnement (LPCE-UJKZ), Burkina Faso through its Director's willingness to collaborate with WASCAL Energy and Climate Change Program of the Abdou Moumouni University, Niamey formerly the University of Niamey, Niger Republic.

Conflicts of Interest

The authors declare no conflicts of interest regarding the publication of this paper.

References

[1] International Energy Agency (2013) Energy Climate and Change. World Energy Outlook Special Report, 1-200.

[2] World Energy Council (2010) 2010 Survey of Energy Resources. http://www.worldenergy.org/

[3] Ramdé, E.W., Azoumah, Y., Brew-Hammond, A., Rungundu, A. and Tapsoba, G. (2013) Site Ranking and Potential Assessment for Concentrating Solar Power in West Africa. *Natural Resources*, **4**, 146-153. https://doi.org/10.4236/nr.2013.41A019

[4] Herrmann, U., Kelly, B. and Price, H. (2004) Two-Tank Molten Salt Storage for Parabolic Trough Solar Power Plants. *Energy*, **29**, 883-893. https://doi.org/10.1016/S0360-5442(03)00193-2

[5] Hoffmann, J. (2015) Stockage thermique pour centrale solaire thermodynamique à concentration mettant en oeuvre des matériaux céramiques naturels ou recycles. Préparée au sein de l'école doctorale: Présentée par Jean-François Hoffmann Stockage thermique pour centrale solairet.

[6] Angelini, G., Lucchini, A. and Manzolini, G. (2014) Comparison of Thermocline Molten Salt Storage Performances to Commercial Two-Tank Configuration. *Energy Procedia*, **49**, 694-704. https://doi.org/10.1016/j.egypro.2014.03.075

[7] Release, P. (2018) The 150 MW Noor Ouarzazate III Solar Tower Power Plant with Storage System Accomplished the First Synchronization.

[8] Libby, C. (2010) Demonstration Development Project: Solar Thermocline Storage Systems: Preliminary Design Study. 188. http://www.epri.com/abstracts/Pages/ProductAbstract.aspx?ProductId=000000000001019581

[9] Ding, W. and Bauer, T. (2021) Progress in Research and Development of Molten Chloride Salt Technology for Next Generation Concentrated Solar Power Plants. *Engineering*, **7**, 334-347. https://doi.org/10.1016/j.eng.2020.06.027

[10] Huang, Q.Z., Lu, G.M., Wang, J. and Yu, J.G. (2011) Thermal Decomposition Mechanisms of $MgCl_2 \cdot 6H_2O$ and $MgCl_2 \cdot H_2O$. *Journal of Analytical and Applied Pyrolysis*, **91**, 159-164. https://doi.org/10.1016/j.jaap.2011.02.005

[11] Pacheco, J.E., Showalter, S.K. and Kolb, W.J. (2001) Development of a Molten-Salt Thermocline Thermal Storage System for Parabolic Trough Plants. *ASME* 2001 *Solar Engineering: International Solar Energy Conference* (*FORUM* 2001: *Solar Energy—The Power to Choose*), Washington, 21-25 April 2001, 453-460. https://doi.org/10.1115/SED2001-158

[12] Kocijel, L., Mrzljak, V. and Glažar, V. (2019) Conversion of a Medium Heavy Heating Oil Tank into A Heat Storage Tank. *Heat and Mass Transfer*, **56**, 871-890. https://doi.org/10.1007/s00231-019-02751-6

[13] Ehtiwesh, I.A.S. and Sousa, A.C.M. (2017) Numerical Model for the Thermal Behavior of Thermocline Storage Tanks. *Heat and Mass Transfer*, **54**, 831-839. https://doi.org/10.1007/s00231-017-2181-6

[14] Kro, D.G. and Kisters, A.F.M. (2014) Solar Energy Materials & Solar Cells Rock Bed Storage for Solar Thermal Power Plants: Rock Characteristics, Suitability, and Availability. *Solar Energy Materials and Solar Cells*, **126**, 170-183. https://doi.org/10.1016/j.solmat.2014.03.030

[15] Ayyappan, S., Mayilsamy, K. and Sreenarayanan, V.V. (2016) Performance Improvement Studies in a Solar Greenhouse Drier Using Sensible Heat Storage Materials. *Heat and Mass Transfer*, **52**, 459-467. https://doi.org/10.1007/s00231-015-1568-5

[16] Laing, D., Steinmann, W.D., Fiß, M., Tamme, R., Brand, T. and Bahl, C. (2008) Solid Media Thermal Storage Development and Analysis of Modular Storage Operation Concepts for Parabolic Trough Power Plants. *Journal of Solar Energy Engineering*, **130**, Article ID: 011006. https://doi.org/10.1115/1.2804625

[17] Geyer, M.A. (1991) Thermal Storage for Solar Power Plants. In: Winter, C.J., Sizmann, R.L. and Vant-Hull, L.L., Eds., *Solar Power Plants*, Springer, Berlin, 199-214. https://doi.org/10.1007/978-3-642-61245-9_6

[18] Agalit, H., Zari, N. and Maaroufi, M. (2017) Thermophysical and Chemical Characterization of Induction Furnace Slags for High Temperature Thermal Energy Storage in Solar Tower Plants. *Solar Energy Materials and Solar Cells*, **172**, 168-176. https://doi.org/10.1016/j.solmat.2017.07.035

[19] Nigay, P.M., Sani, R., Cutard, T. and Nzihou, A. (2017) Modeling of the Thermal and Mechanical Properties of Clay Ceramics Incorporating Organic Additives. *Materials Science and Engineering*: *A*, **708**, 375-382. https://doi.org/10.1016/j.msea.2017.09.131

[20] Razac, A., Nigay, P.-M., *et al.* (2019) An Investigation of the Physical, Thermal and Mechanical Properties of Fired Clay/SiC Ceramics for Thermal Energy Storage. *Journal of Thermal Analysis and Calorimetry*, **140**, 2087-2096. https://doi.org/10.1007/s10973-019-08964-5

[21] Nigay, P., Auteur, A.N., White, C.E. and Soboyejo, W.O. (2019) Structure and Properties of Clay Ceramics for Thermal Energy Storage.

[22] Fasquelle, T., Falcoz, Q., Neveu, P., Walker, J. and Flamant, G. (2017) Compatibility Study between Synthetic Oil and Vitrified Wastes for Direct Thermal Energy Storage. *Waste and Biomass Valorization*, **8**, 621-631. https://doi.org/10.1007/s12649-016-9622-1

[23] Grosu, Y., Ortega-Fernández, I., Del Amo, J.M.L. and Faik, A. (2018) Natural and By-Product Materials for Thermocline-Based Thermal Energy Storage System at

CSP Plant: Compatibility with Mineral Oil and Molten Nitrate Salt. *Applied Thermal Engineering*, **136**, 657-665. https://doi.org/10.1016/j.applthermaleng.2018.03.034

[24] Tiskatine, R. *et al.* (2016) Experimental Evaluation of Thermo-Mechanical Performances of Candidate Rocks for Use in High Temperature Thermal Storage. *Applied Energy*, **171**, 243-255. https://doi.org/10.1016/j.apenergy.2016.03.061

[25] Xu, C., Li, X., Wang, Z., He, Y. and Bai, F. (2013) Effects of Solid Particle Properties on the Thermal Performance of a Packed-Bed Molten-Salt Thermocline Thermal Storage System. *Applied Thermal Engineering*, **57**, 69-80. https://doi.org/10.1016/j.applthermaleng.2013.03.052

[26] Boubou, B., Muritala, I.K., *et al.* (2021) Review on Thermocline Storage Effectiveness for Concentrating Solar Power Plant. *Energy and Power Engineering*, **13**, 343-364. https://doi.org/10.4236/epe.2021.1310024

[27] Ortega-fernández, I., Loroño, I., Faik, A. and Uriz, I. (2017) Parametric Analysis of a Packed Bed Thermal Energy Storage System. *AIP Conference Proceedings*, **1850**, Article ID: 080021. https://doi.org/10.1063/1.4984442

[28] Kenda, E.S., Py, X., N'Tsoukpoe, K.E., Coulibaly, Y. and Sadiki, N. (2018) Thermal Energy Storage Materials Made of Natural and Recycled Resources for CSP in West Africa. *Waste and Biomass Valorization*, **9**, 1687-1701. https://doi.org/10.1007/s12649-017-9904-2

[29] Nitedem, E.K. (2018) Stockage thermique à base d'éco-matériaux locaux pour centrale solaire à concentration: cas du pilote. Spécialité: Energétique et Génie des Procédés Materiaux Locaux Pour Centrale Solaire À Concen.

[30] N'Tsoukpoe, K.E., Azoumah, K.Y., *et al.* (2016) Integrated Design and Construction of a Micro-Central Tower Power Plant. *Energy for Sustainable Development*, **31**, 1-13. https://doi.org/10.1016/j.esd.2015.11.004

[31] Ferber, N.L., Minh, D.P., *et al.* (2020) Development of a Thermal Energy Storage Pressed Plate Ceramic Based on Municipal Waste Incinerator Bottom Ash and Waste Clay.

[32] Fernandez, A.I., Martnez, M., Segarra, M., Martorell, I. and Cabeza, L.F. (2010) Selection of Materials with Potential in Sensible Thermal Energy Storage. *Solar Energy Materials and Solar Cells*, **94**, 1723-1729. https://doi.org/10.1016/j.solmat.2010.05.035

[33] Díaz-Heras, M., Belmonte, J.F. and Almendros-Ibáñez, J.A. (2020) Effective Thermal Conductivities in Packed Beds: Review of Correlations and Its Influence on System Performance. *Applied Thermal Engineering*, **171**, Article ID: 115048. https://doi.org/10.1016/j.applthermaleng.2020.115048

[34] Diago, M., Iniesta, A.C., Delclos, T., Soum-Glaude, A., Shamim, T. and Calvet, N. (2016) Characterization of Desert Sand as a Sensible Thermal Energy Storage Medium. *AIP Conference Proceedings*, **1734**, Article ID: 050011. https://doi.org/10.1063/1.4949109

[35] Diago, M., Iniesta, A.C., Delclos, T., Shamim, T. and Calvet, N. (2015) Characterization of Desert Sand for Its Feasible Use as Thermal Energy Storage Medium. *Energy Procedia*, **75**, 2113-2118. https://doi.org/10.1016/j.egypro.2015.07.333

[36] Bagre, B., *et al.* (2021) Assessment of Different Sands Potentiality to Formulate an Effective Thermal Energy Storage Material (TESM). *SOAPHYS*, 1-7. https://doi.org/10.46411/jpsoaphys.2020.01.08

[37] Sawadogo, M., Seynou, M., *et al.* (2020) Formulation of Clay Refractory Bricks: Influence of the Nature of Chamotte and the Alumina Content in the Clay. *Advances*

in Materials, **9**, 59-67. https://doi.org/10.11648/j.am.20200904.11

[38] Agbo, A., Anene, F. and Nnuka, E. (2017) An Assessment of the Binding Capacity of Bentonite and Ukpor Clay on the Foundry Properties of River Niger, Onitsha Beach Sand. *International Journal of Multidisciplinary Research and Development*, **4**, 26-30. https://www.allsubjectjournal.com/

[39] Sawadogo, Y., Zerbo, L., Sawadogo, M., Seynou, M., Gomina, M. and Blanchart, P. (2020) Characterization and Use of Raw Materials from Burkina Faso in Porcelain Formulations. *Results Mater*, **6**, Article ID: 100085. https://doi.org/10.1016/j.rinma.2020.100085

[40] Iniesta, A.C., Diago, M., Delclos, T., Falcoz, Q., Shamim, T. and Calvet, N. (2015) Gravity-Fed Combined Solar Receiver/Storage System Using Sand Particles as Heat Collector, Heat Transfer and Thermal Energy Storage Media. *Energy Procedia*, **69**, 802-811. https://doi.org/10.1016/j.egypro.2015.03.089

[41] Savadogo, N. (2017) Élaboration et caractérisation d' un écociment à base de poudre de mâchefer de charbon mineral. Élaboration et caractérisation d' un écociment à base de poudre de mâchefer de charbon, 187.

[42] Boubou, B., Kolawole, M.I., *et al.* (2021) Assement of Different Sands Potentiality to Formulate and Effective Thermal Energy Storage Material (TESM). *Soaphys*, **2**, 1-7. https://doi.org/10.46411/jpsoaphys.2020.01.08

[43] De Noni, A., Hotza, D., Soler, V.C. and Vilches, E.S. (2010) Influence of Composition on Mechanical Behaviour of Porcelain Tile. Part I: Microstructural Characterization and Developed Phases after Firing. *Materials Science and Engineering*: *A*, **527**, 1730-1735. https://doi.org/10.1016/j.msea.2009.10.057

[44] Hoffmann, J.-F. Fasquelle, T. Goetz, V. and Py, X. (2016) A Thermocline Thermal Energy Storage System with Filler Materials for Concentrated Solar Power Plants: Experimental Data and Numerical Model Sensitivity to Different Experimental Tank Scales. *Applied Thermal Engineering*, **100**, 753-761. https://doi.org/10.1016/j.applthermaleng.2016.01.110

[45] Ormerod, A. (1961) Measurement of the Tensile Strength of Brittle Materials. *British Journal of Applied Physics*, **12**, 29-30. https://doi.org/10.1088/0508-3443/12/1/108

[46] Jaeger, J.C. (1967) Failure of Rocks under Tensile Conditions. *International Journal of Rock Mechanics and Mining Sciences & Geomechanics Abstracts*, **4**, 219-227. https://doi.org/10.1016/0148-9062(67)90046-0

[47] Salençon, J., Hiramatsu, Y. and Okavol, Y. (1967) Determination of the Tensile Strength of Rock by a Compression Test of an Irregular Test Piece. *International Journal of Rock Mechanics and Mining Sciences & Geomechanics Abstracts*, **4**, 363-365. https://doi.org/10.1016/0148-9062(67)90017-4

[48] Pejchal, V., Žagar, G., Charvet, R., Dénéréaz, C. and Mortensen, A. (2017) Compression Testing Spherical Particles for Strength: Theory of the Meridian Crack Test and Implementation for Microscopic Fused Quartz. *Journal of the Mechanics and Physics of Solids*, **99**, 70-92. https://doi.org/10.1016/j.jmps.2016.11.009

[49] Miserez, A. and Mortensen, A. (2004) Fracture of Aluminium Reinforced with Densely Packed Ceramic Particles: Influence of Matrix Hardening. *Acta Materialia*, **52**, 5331-5345. https://doi.org/10.1016/j.actamat.2004.07.038

[50] Devices, D. (2016) KD2 Pro Thermal Properties Analyzer.

[51] Ferber,N.L., Minh, D.P., *et al.* (2020) Development of a Thermal Energy Storage Pressed Plate Ceramic Based on Municipal Waste Incinerator Bottom Ash and Waste Clay. *Waste and Biomass Valorization*, **11**, 689-699.

https://doi.org/10.1007/s12649-019-00629-6

[52] Balogun, O.A., Akinwande, A.A., *et al.* (2021) Experimental Study on the Properties of Fired Sand-Clay Ceramic Products for Masonry Applications. *Journal of Materials in Civil Engineering*, **33**, 1-12. https://doi.org/10.1061/(ASCE)MT.1943-5533.0003532

[53] Bennour, A., Mahmoudi, S., Srasra, E., Boussen, S. and Htira, N. (2015) Composition, Firing Behavior and Ceramic Properties of the Sejnène Clays (Northwest Tunisia). *Applied Clay Science*, **115**, 30-38. https://doi.org/10.1016/j.clay.2015.07.025

[54] Da Silva, A.M.F.D., Toledo, R., *et al.* (2014) Influence of Firing Temperature on the Behavior of Clay Ceramics Incorporated with Elephant Grass Ash. *Materials Science Forum*, **798-799**, 526-531. https://doi.org/10.4028/www.scientific.net/MSF.798-799.526

[55] Yilmaz, S. (2018) Creep of Hard Porcelain during Firing, No. 49081.

[56] Homand-Etienne, F. and Houpert, R. (1989) Thermally Induced Microcracking in Granites: Characterization and Analysis. *International Journal of Rock Mechanics and Mining Sciences & Geomechanics Abstracts*, **26**, 125-134. https://doi.org/10.1016/0148-9062(89)90001-6

[57] Bougara, U.M.H. (2013) Evaluation des propriétés réfractaires et cimentaires du kaolin de Djebel Debbagh Remerciements. Thèse de Doctorat, Faculté des sciences de l'ingénieur, Boumerdes.

[58] Michot, A., Smith, D.S., Degot, S. and Gault, C. (2008) Thermal Conductivity and Specific Heat of Kaolinite: Evolution with Thermal Treatment. *Journal of the European Ceramic Society*, **28**, 2639-2644. https://doi.org/10.1016/j.jeurceramsoc.2008.04.007

[59] Bayón, R. Rivas, E. and Rojas, E. (2014) Study of Thermocline Tank Performance in Dynamic Processes and Stand-By Periods with an Analytical Function. *Energy Procedia*, **49**, 725-734. https://doi.org/10.1016/j.egypro.2014.03.078

[60] Bwayo, E. and Obwoya, S.K. (2014) Coefficient of Thermal Diffusivity of Insulation Brick Developed from Sawdust and Clays. *Journal of Ceramics*, **2014**, Article ID: 861726. https://doi.org/10.1155/2014/861726

[61] Gil, A., Medrano, M., *et al.* (2010) State of the Art on High Temperature Thermal Energy Storage for Power Generation. Part 1—Concepts, Materials and Modellization. *Renewable and Sustainable Energy Reviews*, **14**, 31-55. https://doi.org/10.1016/j.rser.2009.07.035

Nomenclature

DNI Direct Normal Irradiance (5.5 $kWh \cdot m^{-2} \cdot day^{-1}$)
TES thermal energy storage
CSP Concentrating Solar Power
PV Photovoltaic
SONICHAR Société Nigérienne de Charbon
A bottom ash sample
C clay sample from the deposit of Malgsombo in the commune of Saaba
C1 clay sample the deposit of Ethouayou in the commune of Tcheriba
DS-B dune sand from Burkina Faso
DS-N Dune sand from Niger
MS-B Mining sand from Burkina Faso
NS-N Natural sand from Niger
D dune sand sample in the ceramic ball
M Mining sand sample in the ceramic ball
N Natural sand sample in the ceramic ball
K is a numerical constant
LOI Lost on ignition
m_0 specimen mass after drying in the oven [g]
m_1 specimen mass after firing in the muffle furnace [g]
x value obtained by test
$\overline{x}$ the average of measurement values
n total number of test
SE standard error [%]
c_p specific heat capacity [J/kg·˚C]
F_f the peak load at failure of the sphere or the ceramic ball [N]
R the radius of the sphere or the ceramic ball [m]
d thermal diffusivity [$mm^2 \cdot s^{-1}$]
SHS Sensible heat storage
TESM Thermal Energy Storage Materials

Greek abbreviation

σ_t tensile strength [Pa]
λ thermal conductivity [$Wm^{-1} \cdot K^{-1}$]
ε specimen or ceramic ball porosity [%]

Subscript

dryspecimen weight in air dry specimen mass taken in air
specimen weight in water specimen mass taken in water
b ball
w water
t tensile
i number of test
p constant pressure or isobar condition